Journal of Hydrology 615 (2022) 128687

Contents lists available at ScienceDirect

Journal of Hydrology

journal homepage: www.elsevier.com/locate/jhydrol

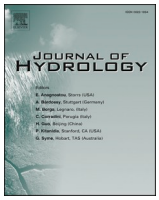

Research papers

A new framework for flood damage assessment considering the within-event time evolution of hazard, exposure, and vulnerability

Tommaso Lazzarin [a,*], Daniele P. Viero [a], Daniela Molinari [b], Francesco Ballio [b], Andrea Defina [a]

[a] Department of Civil, Environmental and Architectural Engineering, University of Padova, Italy
[b] Department of Civil and Environmental Engineering, Politecnico di Milano, Italy

ARTICLE INFO

Editor: Yuefei Huang
Associate Editor: Chunhui Lu

Keywords:
Damage
Flood
Exposure
Hazard
Vulnerability
Flood risk

ABSTRACT

Commonly adopted procedures for flood damage assessment are based on functions of the hazard that depend on the item under investigation (e.g., an area, a building), and on the vulnerability of exposed items. Available flood damage models make use of summary indicators, usually correspondent to the worst conditions expected during the flood event (e.g., the maximum flooded area, the envelop of maximum water depths, the maximum presence of people in the area, etc.), which cannot properly describe the time evolution of hazard and exposure during the flood event. This is an important limitation, as the flood damage also depends on how the involved processes evolve in time. In the present work, we propose a new framework for the assessment of flood damage that considers how damage evolves in time within a single flood event. The goal is achieved by computing flood damage by integrating over time the rate at which damage progresses, which in turn depends on time-varying hydraulic conditions and exposure. Application to schematic, yet realistic, examples shows the effectiveness of the method and its potential in flood risk assessment and management.

1. Introduction

With the shift from "hazard control" to "integrated risk management", the estimation of flood damage has gained increased importance in the last decades, as the base for the evaluation of costs and benefits of risk mitigation actions, both in the peace time and during the emergency. At the same time, flood damage modelling capability increased as well. Starting from the simple concept of "depth-damage curve" introduced in the fifties for the estimation of flood damage to residential buildings (White, 1945, 1964), flood damage models have progressively improved resulting in the current availability of more comprehensive and complex estimation tools. On the one hand, research on flood damage expanded to include the main typologies of exposed assets: flood damage models are now available for assessing damage to people (e.g., Arrighi et al., 2017; Cox et al., 2010; Milanesi et al., 2015; Ramsbottom et al., 2006), vehicles (e.g., Arrighi et al., 2015; Bocanegra et al., 2020; Martínez-Gomariz et al., 2018; Milanesi and Pilotti, 2019; Shand et al., 2011), crops (e.g., Dutta et al., 2003; Molinari et al., 2019; Shrestha et al., 2016), commercial/industrial premises (e.g., Gissing and Blong, 2004; Kreibich et al., 2010), infrastructures (e.g., Gallazzi et al., 2021; Kramer et al., 2016; Pregnolato et al., 2017), and cultural heritage (e.g., Arrighi et al., 2018; Figueiredo et al., 2021). On the other hand, complexity of models increased, although in an unbalanced way for the different exposed assets (with the residential sector being the most investigated one). Multi-variable models have been developed, allowing to consider the role of several hazard and vulnerability variables in shaping damage, besides the one played by water depth. With respect to the hazard, models are now available to consider the combined effect of water depth, water velocity, water contamination, and flood duration (Brémond et al., 2013; Chen et al., 2016; de Moel and Aerts, 2011; Merz et al., 2010; Pita et al., 2021). Likewise, most of existing damage models allow including at least one significant vulnerability variable, with the number and typology of them strongly depending on the asset under investigation (see Gerl et al., 2016 for an overview). Literature on flood damage modelling is unambiguous in evaluating multi-variable models as outperforming simple uni-variable tools, such as depth-damage functions (Carisi et al., 2018; Schröter et al., 2014; Wagenaar et al., 2017). Still, the calibration and implementation of multi-variable models are often hampered by the paucity of reliable data. For example, it is not always straightforward to evaluate hazard variables such as flood duration and contamination, or to acquire sufficiently accurate information, e.g., on vulnerability of the ground floor of

* Corresponding author.
E-mail address: tommaso.lazzarin@phd.unipd.it (T. Lazzarin).

https://doi.org/10.1016/j.jhydrol.2022.128687
Received 22 July 2022; Received in revised form 30 September 2022; Accepted 21 October 2022
Available online 9 November 2022

buildings, on physical characteristics of exposed people, on types of crops, etc. The increased availability of ex-post damage data and innovative modelling techniques like Bayesian frameworks, machine learning algorithms, etc., promoted then the development of advanced probabilistic approaches that allow to consider uncertainty of both input data and damage mechanisms (Carisi et al., 2018; Kreibich et al., 2017; Lüdtke et al., 2019; Sairam et al., 2020).

Despite the strong heterogeneity of current flood damage models, in terms of investigated assets, number of input variables, and modelling approaches, available models all disregard the time-evolution of the damaging processes within the flood event. They estimate the damage as a function of fixed values of the input variables (being them related to hazard, exposure, or vulnerability), usually corresponding to the worst conditions expected during a flood (the maximum water depth and velocity, the maximum exposure, etc.). In other words, a time-dependent problem is reduced to the estimation of the final state of damage as a function of some summary indicators that briefly describe the hazard and exposure associated to a flood event. Here we question the general validity of this paradigm, as neglecting the time evolution of the multiple and complex processes that produce the flood damage is likely oversimplified. Estimating the damage by considering the time evolution of the flood characteristics, and hence of the hazard variables, as well as how exposure and vulnerability change during the flood event, is more adherent to reality, and likely more appropriate and effective than the standard approach. This is the reason why we propose a model for direct damage assessment that explicitly considers the temporal evolution of the flooding characteristics, as well as those of exposure and vulnerability scenarios.

While entailing an increased number of parameters with associated uncertainties, the new framework paves the way to a wealth of promising applications. For example, it may allow *i*) to estimate flood damage more accurately in cases of markedly time-varying hazard and/or time-dependent exposure and vulnerability scenarios, *ii*) to estimate the effectiveness of disaster countermeasures and civil protection activities that can be undertaken in the course of a flood event in order to rescue and protect human lives and properties, and *iii*) to explicitly evaluate the advantages related to the availability and reliability of real-time flood forecasts.

The proposed model is described in Section 2. Section 3 presents and discusses some examples of model application aiming at providing information about the model capability in predicting the damage produced by flood events, rather than supporting a validation of the model for the selected assets. Some additional remarks and a set of conclusions close the paper.

2. The mathematical model

The model aims at describing the time-evolution of damage within a single flood event, as driven by the time-varying flood hazard, which is the independent variable of the problem. The model is spatially distributed in its nature and is meant to estimate the local damage as the sum of damage suffered by homogeneous categories of items exposed to flooding. This means that the overall damage is obtained by summation on the exposed item categories and by spatial integration on the flooded area. Hereinafter, the model structure is explained with reference to a single item category and to a generic point $\mathbf{x} = (x, y)$ within the flooded area (i.e., the dependence of variables on position $\mathbf{x}$ and on the specific item category is implicitly assumed).

The basic idea is that items exposed to flooding are progressively "eroded" by the flood. This can be the case of the many categories of assets for which damage progresses gradually (e.g., buildings). However, this damage mechanism can be extended also to the case of objects that can be either safe or fully damaged (hereinafter denoted as on/off objects) when they are hit by floodwaters, by considering the damaging process from a statistical point of view. In case of on/off items, the vulnerability of the object is the probability of being fully damaged when stressed by a constant hydrodynamic forcing (Lazzarin et al., 2022). This probability typically increases with the time the object is exposed to the flow; therefore, we may also consider on/off objects as gradually eroded by the flood. A representative category of on/off objects is that of people; the probability of being swept away by floodwaters depends on the duration of the flooding because, *i*) the longer a person remains in floodwaters, the smaller is his resistance, and *ii*) the probability of being hit by large scale, energetic turbulent flow events, not resolved by the hydrodynamic model, or, e.g., by floating debris, increases with time.

2.1. The model variables

In the model, the intensity of the hydrodynamic forcing (i.e., the hazard) at a given location, as it varies in time, is measured using a single parameter, $W = W(t)$. For instance, a basic choice would be assuming W equal to the water depth. Here we choose the W parameter proposed by Lazzarin et al. (2022), which stems from a combination of flow mechanical energy per unit weight, and momentum per unit width and specific weight. It is written as

$$W = \left(\frac{Y}{Y_W}\right)^{\alpha}\left(1+\beta F^2\right) \text{ with } Y_W > 0, \alpha \geq 1, \beta \geq 0 \tag{1}$$

in which $F = U(gY)^{-1/2}$ is the Froude number (with Y the water depth and U the flow velocity), Y_W is a reference depth introduced to scale the water depth, and α and β are two calibration factors that measure the relative importance of static versus dynamic energy/force component. It is worth noting that W can recover the water depth, Y ($Y_w = 1$, $\alpha = 1$ and $\beta = 0$), the flow energy per unit weight, H ($Y_w = 1$, $\alpha = 1$ and $\beta = 0.5$), and the momentum per unit width and specific weight, M ($Y_w = \sqrt{2}$, $\alpha = 2$ and $\beta = 2$) by suitably choosing the reference depth and the two calibration factors (Lazzarin et al., 2022).

We denote with $\mathbb{E}_0$ the quantity, or the value, of potentially exposed items, belonging to a single homogeneous category, present in a unit area at the initial time t_0. For instance, $\mathbb{E}_0$ may be the number of exposed people or the economic value of exposed buildings. Such quantity/value can reduce in time due to countermeasures and rescue activities performed in the course of the flood event and is denoted by $\mathbb{E} = \mathbb{E}(t)$. We then introduce the following non-dimensional, time-dependent, "specific" variables that range in the interval [0,1]:

- the damage, $D = D(t)$, which is the damaged fraction of $\mathbb{E}$ at time t;
- the vulnerability, $V(W)$, which is here defined to be the fraction of $\mathbb{E}$ that can be damaged if subject to constant hydrodynamic forcing, W, lasting for a reasonably long period of time. Since W depends on time, vulnerability depends on/changes in time as well. $V(W)$ can be interpreted as the potential damage associated to the given hazard degree;
- the rescue function, $R = R(t)$, which is the fraction of $\mathbb{E}_0$ that has been rescued.

The meaning of these variables is clarified in the schematics of Fig. 1. We stress that all variables actually depend on the position, $\mathbf{x}$, and provide the spatial distribution of hazard, exposure, vulnerability, outcome of rescue activities, and damage.

2.2. The model equations

The model is built upon a basic conservation principle applied to items exposed to flooding. The quantity (or the value) of potentially exposed items, as it decreases in time depending on the rescue function, is expressed as

$$\mathbb{E} = \mathbb{E}_0[1 - R] \tag{2}$$

Given that damaged items cannot be rescued any more, R in Eq. (2)

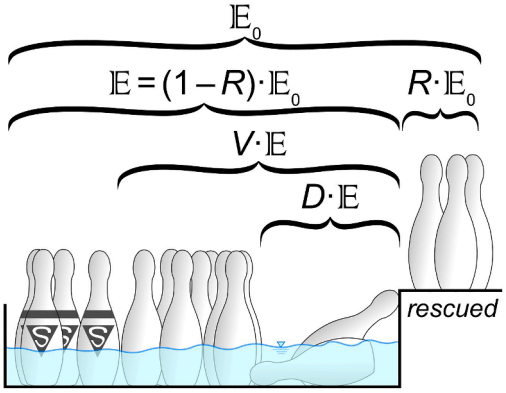

Fig. 1. Schematic representation of items, mimicked by skittles, exposed to floodwaters (pale blue) and of the relevant model parameters and functions. The skittles marked with "S" are strong enough to resist to the current hazard degree. (For interpretation of the references to colour in this figure legend, the reader is referred to the web version of this article.)

must satisfy the constraint $R \leq 1 - D \bullet \mathbb{E}/\mathbb{E}_0$, possibly limiting the rescue. The rescue function, R, depends on several factors: the kind of asset under investigation, the hydrodynamic forcing, and external factors such as the availability and efficiency of rescue services (Kienzler et al., 2015; Thieken et al., 2007). The key dependence of R on external factors makes it extremely case-dependent, thus unsuitable for a general, theoretical assessment.

The core of the model is predicting the growth of damage in time, $D(t)$, as a function of the hydrodynamic forcing, i.e., of the hazard degree $W(t)$. Typically, for a generic object affected by flooding, the early stage of damaging starts slowly, then develops faster and faster. This is because an exposed item has an initial resistance that progressively reduces; in fact, with the damaging process progressing, exposed objects weaken and hence become more susceptible to being damaged. On the contrary, at the later stage of the process, damaging slows down and the maximum damage is reached gradually (Breaden, 1971); at this stage, the damaging rate becomes nearly proportional to the undamaged fraction of the objects effectively exposed to the action of floodwaters, $V - D$ (Fig. 1), scaled by the relative potential damage, V. Mathematically, this behaviour can be described by the following equation

$$\frac{d}{dt}(D\mathbb{E}) = cD\mathbb{E}\left(1 - \frac{D}{V}\right) \tag{3}$$

with c a damage rate factor that controls the speed at which the damage progresses. Reasonably, the damage rate factor increases with the hazard increasing, making $c = c(W)$ a monotone increasing function.

The above equation belongs to the family of the so-called logistic equations, with the damaged items $D \bullet \mathbb{E}$ corresponding to a growing population, and the maximum quantity of damageable items, $V \bullet \mathbb{E}$, corresponding to the so-called *carrying capacity* (i.e., the maximum population size compatible with external constraints; Chapman and Byron, 2018).

As the flood evolves in times, particularly during the receding phase when $W(t)$ becomes gradually smaller, the fraction of potentially damageable items, $V(W)$, may reduce to values smaller than the current damage, $D(t)$, whereas Eq. (3) is strictly valid when $V \geq D$. To account for this, and to extend the adaptability of the proposed equation to a wider range of cases, we rewrite Eq. (3) in the more general form

$$\frac{d}{dt}(D\mathbb{E}) = \mathbb{E} \bullet cD^{1-\gamma}\left(1 - \frac{D}{max(V,D)}\right)^{1+\gamma} \tag{4}$$

with γ a calibration parameter in the range $0 \leq \gamma \leq 1$. When $\gamma = 0$, the solution to Eq. (4) is the well-known logistic function. As γ increases, the duration of the initial stage of fast damaging reduces (see Sect. 2.3.1). As a first approximation, γ is here assumed to be constant for a given category of exposed assets, as the initial delay at which damage begins to develop mainly depends on the characteristics of assets rather than on hazard intensity.

The logistic equation in the differential form, Eq. (4), along with Eq. (2), allows predicting the evolution of D. Once the model parameters have been assessed, Eq. (4) can be integrated, at each point $\mathbf{x}$ within the flooded area, with any simple numerical approach (e.g., finite difference) using the results $Y(\mathbf{x},t)$ and $U(\mathbf{x},t)$, and hence $W(\mathbf{x},t)$, provided by suitable hydrodynamic models. Specific damage times the potential exposure, $D(\mathbf{x},t) \bullet \mathbb{E}(\mathbf{x},t)$, gives the spatial distribution of the damage per unit area. Integration over the flooded area yields the time-evolution of the damage and, at the end of the flood event, the total damage.

Hereinafter, for a general assessment of the model, we assume that the rescue function is identically zero, so that the potential exposure is constant in time, i.e., $\mathbb{E}(t) = \mathbb{E}_0$. The logistic equation then reduces to

$$\frac{dD}{dt} = cD^{1-\gamma}\left(1 - \frac{D}{max(V,D)}\right)^{1+\gamma} \tag{5}$$

which has a close form analytical solution if V is constant in time, which corresponds to assuming a constant hazard degree, W.

2.3. Assessment of model parameters and functions

To estimate the time evolution of the damage, $D(t)$, for each asset category, the parameters and variables appearing in Eq. (5) need to be evaluated by calibration using available experimental data, information, and/or phenomenological models. Considering that γ can be taken as a constant parameter, whereas c and V actually depend on the impact parameter, W, calibrating the model means determining one parameter, γ, and two univariate functions, $c = c(W)$ and $V = V(W)$.

As the procedure to calibrate the model parameters is different for the categories of gradually damaging assets and on/off objects, they are dealt with separately in the next sections.

2.3.1. The case of gradually damaging assets

In order to determine γ, c, and V for a given asset category, we use the solution of Eq. (5) when W is constant in time, so that $c(W)$ and $V(W)$ turn out to be constant as well. By prescribing $D = 0$ when $t = 0$, the solution of Eq. (5) reads

$$D(t) = \frac{V}{1 + V \bullet (c\gamma\, t)^{-1/\gamma}} \tag{6}$$

Assuming a constant value of W is convenient because available information and data on gradually damaging assets typically refer to constant hydraulic forcing, which means knowing the damage produced by constant values of W for different flood durations, τ. Yet, in this case the time t coincides with the flood duration, τ, and hence $D(t) \equiv D(\tau)$.

Close inspection of Eq. (6) shows that c controls the speed at which the damage progresses. Fig. 2a shows that, during the early stage of the damaging process, dD/dt increases with c increasing. For a given value of c, γ controls the delay with which damage starts increasing, that is, the smaller is γ, the more delayed is the damaging process (Fig. 2b). These behaviors can be of help in calibrating c and γ.

The calibration procedure is outlined as follows:

1. the first preliminary step is assessing the structure of the impact parameter W to describe the hydrodynamic forcing by means of a single parameter (Lazzarin et al., 2022);
2. a set of damage values, D, at different times, t, and for different values of W, is extracted from available data;
3. for each value of W, the best fit of Eq. (6) to the (D, t) couples provides a set of (c, W) and (V, W) couples, as well as an estimate of the parameter γ;

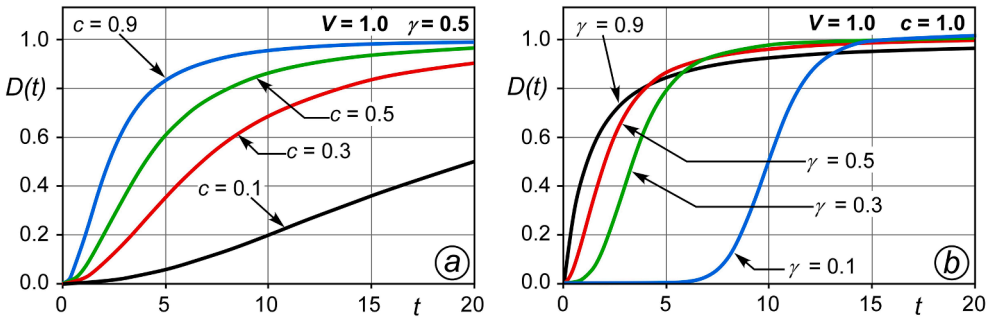

Fig. 2. Time evolution of the specific damage, $D(t)$, according to Eq. (6), for $V = 1$ and: a) for different values of the damaging rate, c (with $\gamma = 0.5$); b) for different values of γ (with $c = 1$).

4. finally, the functions $c(W)$ and $V(W)$ can be obtained by interpolating the set of (c, W) and (V, W) couples, respectively.

The above procedure is applied in the two examples of Sections 3.1 and 3.2, for the sake of illustration.

2.3.2. The case of on/off damaging objects

For on/off objects, $V(W)$ is actually the probability of occurrence of an off-event. For example, for the category of people, vulnerability is the probability of being swept away by floodwaters of given depth and velocity, hence W; this probability depends on many factors such as weight, height, sex, age, clothes, physical condition, as well as on ground topography and, why not, on fate (Arrighi et al., 2017; Jonkman and Penning-Rowsell, 2008; Lind et al., 2004). Accordingly, $V(W)$ can be assessed using a statistical approach based on a significant set of off-event data and the corresponding W values; $V(W)$ is then given by the cumulative distribution function (CDF) of W associated to the off-events. A more detailed description of this procedure is given by Lazzarin et al. (2022).

Finding a suitable relationship for the damaging rate factor, $c(W)$, is not straightforward, as it is affected by manifold aspects. Off events in floodwaters can be triggered by strong macroturbulent events, as well as by floating and suspended debris; hence, the probability of occurrence of an off-event (i.e., the damage) increases as time passes. In addition, for some on/off objects, like people or animals, fatigue plays a role as well. Anyway, the damaging process for on/off objects is typically fast compared to the flooding time scale, so that approximations affecting the estimation of $c(W)$ have a minor impact on the accuracy of model predictions (see Section 3).

For on/off damaging objects, the procedure to calibrate the model is summarized as follows:

1. the first preliminary step is assessing the structure of the impact parameter W (Lazzarin et al., 2022);
2. then, available data are used to provide a statistically significant set of W values corresponding to off-events. The cumulative distribution of W values provides the vulnerability function $V(W)$;
3. the damage rate factor $c(W)$ can be inferred by a best fit of Eq. (6) to available experimental data; in the absence of experimental data or theoretical evaluations, a possible, reasonable function $c(W)$ should be assumed.

The above procedure is applied in the example of Section 3.3 for the sake of illustration.

3. Model applications

Of the three illustrative applications shown in this section, the first two examples consider crops and buildings as gradually damaging assets; the third example, that considers the category of people, shows how the procedure is extended to an on/off object category.

The purpose of the examples discussed in this section is to exemplify the above calibration procedure and to show the model ability in describing the time-evolution of damage as determined by the time-varying flow conditions that occur in the course of a synthetic flood event. The present model applications also suggest the importance of considering the evolution of the damaging process for an improved assessment of flood risk. The application to a real flood event, with inclusion of the rescue function, is beyond the scope of the present methodological study.

In real-case modelling applications, the results from a hydrodynamic model provide the spatial distribution of water depth and velocity within the flooded area as they vary in time during the flood event. Such data allows computing the spatial and temporal distribution of the impact parameter, W, for each investigated category of exposed assets, by means of Eq. (1). How to assess the W parameter to actually represent the hazard degree for different object categories is described in Lazzarin et al. (2022). Here, for the sake of the exercise, we consider a generic spatial position within the flooded area, and we introduce some synthetic hydrographs describing the local time variation of W. The selected hydrographs, shown in Fig. 3, have different shapes but the same peak value.

3.1. Flood damage to crops

Flood duration is one of the key explicative variable of flood damage to crops (Berning et al., 2000; Forster et al., 2008; Mao et al., 2016; Merz et al., 2010; Scawthorn et al., 2006; Vozinaki et al., 2015) as plants resist differently to ponding water persisting few hours rather than several days. In fact, most of the existing models for estimating flood damage to agriculture consider flood duration as an important explicative variable complementing the maximum flow depth (e.g., Agenais et al., 2013;

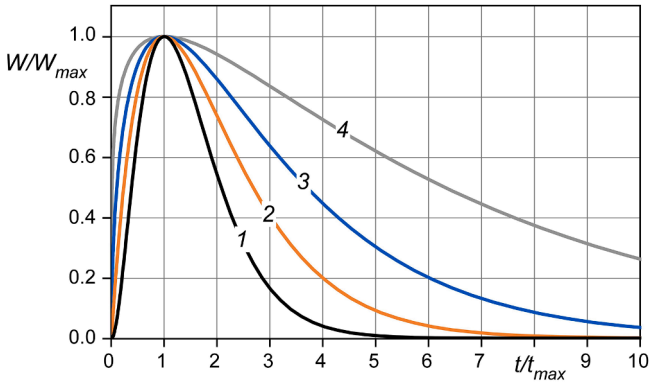

Fig. 3. Synthetic hydrographs describing the time variation of W used in the present model application examples; labels 1 to 4 denote the different shape of hydrographs; W_{max} is the peak value of W and t_{max} the time to peak.

Brémond et al., 2013; Dutta et al., 2003; Molinari et al., 2019). Nevertheless, the dynamics of flood damage mechanisms is not considered by the models; with the proposed approach, the temporal evolution of the flood is instead implicitly accounted for, as demonstrated by the following examples.

Among crops, we choose rice as its damaging is perhaps the most well documented (e.g., Khairul et al., 2022; Nguyen et al., 2021; Samantaray et al., 2015; Singh et al., 2011; Zhang et al., 2015). In particular, we use the data and damage functions for rice at maturity stage, as given by Shrestha et al. (2016). Given that the damage is given as a function of water depth in this model, we assume $\alpha = 1$, $\beta = 0$, and $Y_W = 1.0$ m in Eq. (1), so that W exactly corresponds to the water depth. According to the model by Shrestha et al. (2016), the damage attains the maximum value when $W > 1.2$ (Fig. 4a), and it strongly depends on the duration of the flood.

The model calibration, which means determining γ, $c(W)$, and $V(W)$, is based on the use of Eq. (6), which holds when the impact parameter $W(t)$ is constant in time. Accordingly, we extract from the data of Fig. 4a all the couples (D, τ) for some constant values of W. These set of iso-W data (dots in Fig. 4b) is fitted with Eq. (6) (lines in Fig. 4b) to find $\gamma = 0.6$ and the values of vulnerability and damage rate factor reported in Table 1.

The next step is obtaining suitable expressions for $V(W)$ and $c(W)$. Valid possibilities are interpolating the data of Table 1 with a piecewise linear function, or using a higher order polynomial approximation. An effective solution is using suitable algebraic expressions containing few calibration factors, as those reported in the following equations:

$$V(W) = \frac{1}{1 + (a/W)^b} \tag{7}$$

$$c(W) = pW^q \tag{8}$$

where a, b, p, and q are calibration coefficients.

For rice during the maturity stage (data in Table 1), the vulnerability function $V(W)$ is well described by $a = 0.85$ and $b = 7$ (Fig. 5a), and the damage rate factor $c(W)$ by $p = 0.4$ d^{-1} and $q = 1.5$ (Fig. 5b).

Once calibrated, the model is used to predict the damage produced by the synthetic flood events of Fig. 3, by integrating Eq. (5). The results, obtained by assuming $t_{max} = 1$ d, are shown in Fig. 6a for $W_{max} = 1.5$, and in Fig. 6b for $W_{max} = 1.0$. We recall that, in this specific application, the W parameter represents the water depth expressed in meters.

Both in the case of $W_{max} = 1.5$ and $W_{max} = 1.0$, in the rising phase of the flood, the damage increases slowly, with a temporal evolution that is almost the same for the different hydrographs. For the longest flood (labelled as 4) and $W_{max} = 1.5$, the damage is smaller than 20% at the flood peak. In the receding phase (i.e., for $t > 1$ day), in the steeper hydrograph (labelled as 1), water levels decrease fast and, after approximatively $t = 2$ days, damage does not increase anymore, reaching $D = 0.32$ and $D = 0.11$ for $W_{max} = 1.5$ and of $W_{max} = 1.0$ respectively. For the longest hydrograph (labelled as 4), relatively high water depths last for several days after the peak, and damage continues to increase until $t = 5$ days for $W_{max} = 1.5$ (where $D = 0.63$) and $t = 3$ days for $W_{max} = 1.0$ (where $D = 0.27$). Hence, the hydrograph n. 4 produces a final damage approximately two times higher than hydrograph n. 1, due to the longer persistence of high water levels.

Table 1
Model parameters V and c obtained from data in Shrestha et al. (2016) for some values of the impact parameter W.

W	0.6	0.7	0.8	0.9	1.0	1.1	1.2
V	0.16	0.30	0.44	0.58	0.72	0.86	0.99
c [d^{-1}]	0.14	0.23	0.30	0.37	0.42	0.48	0.53

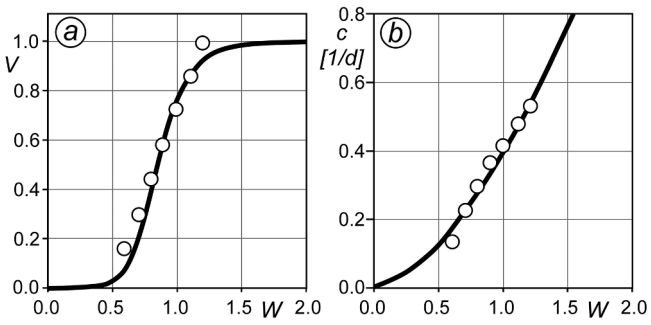

Fig. 5. Vulnerability, $V(W)$, and damage rate, $c(W)$, according to Eqs. (7) with $a = 0.85$, $b = 7$, and to Eq. (8) with $p = 0.4$ d^{-1}, $q = 1.5$, respectively. White dots denote the (V, W) and (c, W) couples of Table 1.

Model parameters are also evaluated for the three growing stages of rice: vegetative (i.e., after newly planted), reproductive, and maturity stage. We followed the same calibration procedure outlined for the maturity stage, using data of Shrestha et al. (2016). Interestingly, while vulnerability shows a marked dependence on the growing stage (Fig. 7a), the damage rate factor, $c(W)$, is approximately the same for the three stages (Fig. 7b).

Finally, we use the model of Agenais et al. (2013) to consider other crops. Specifically, we consider grapevine and maize, both at the maturity stage, and compare the time evolution of the specific damage, $D(t)$, with those obtained for rice using the hydrograph 4 of Fig. 3 with $t_{max} = 1$ day and $W_{max} = 1.5$. The damaging of grapevine and maize shows a different temporal evolution compared to rice (Fig. 8): the initial stage of the damaging process is delayed; however, damage progresses faster in time and the final value is higher, particularly for grapevine crops, which is characterized by a lower value of γ and a

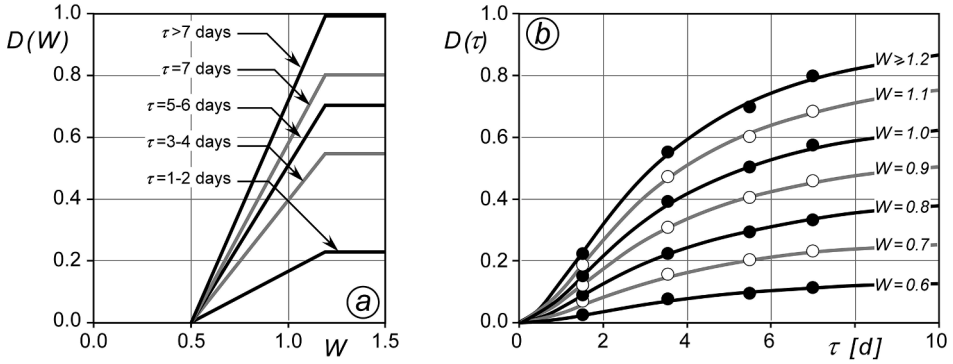

Fig. 4. Damage to rice during the maturity stage, expressed as relative yield loss, a) as a function of the impact parameter W, for different flood durations τ (adapted from Shrestha et al., 2016), and (b) as a function of the flood duration, τ, for different values of W; dots denote the discrete values extracted from the curves plotted in (a). The iso-W curves in (b) are computed with equation Eq. (6) with $t = \tau$.

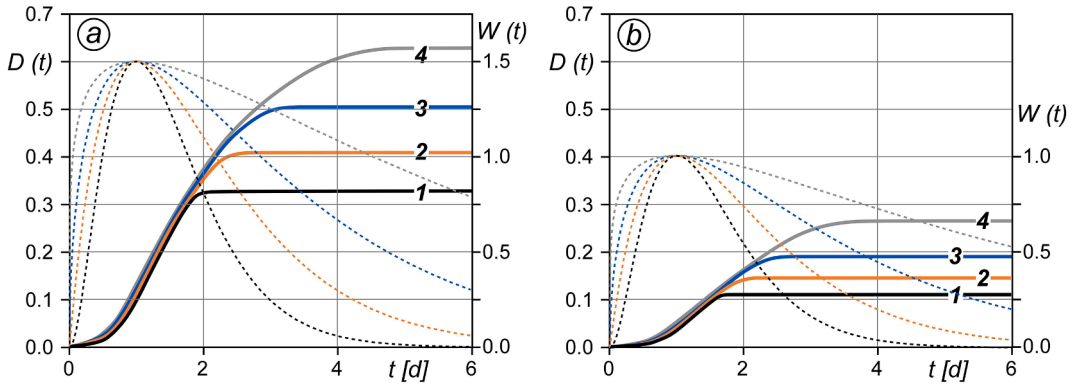

Fig. 6. Specific damage growth for rice, $D(t)$, (solid lines) subject to the different flood hydrographs $W(t)$ shown in Fig. 3 (dashed lines), with $t_{max} = 1$ day and a) $W_{max} = 1.5$, b) $W_{max} = 1.0$.

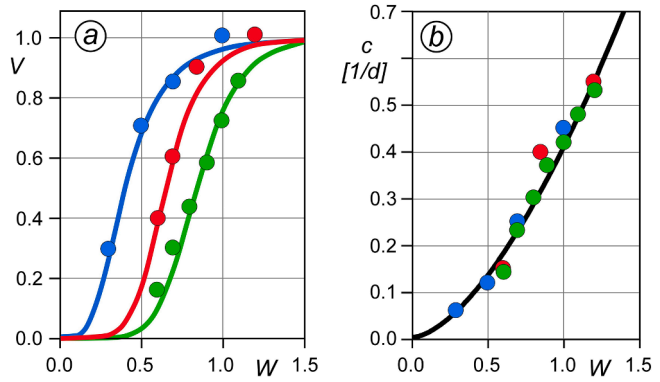

Fig. 7. Vulnerability $V(W)$ given by Eq. (7) and b) damage rate factor $c(W)$ given by Eq. (8) for rice at different growing stages: vegetative (blue), reproductive (red), and maturity stage (green). (For interpretation of the references to colour in this figure legend, the reader is referred to the web version of this article.)

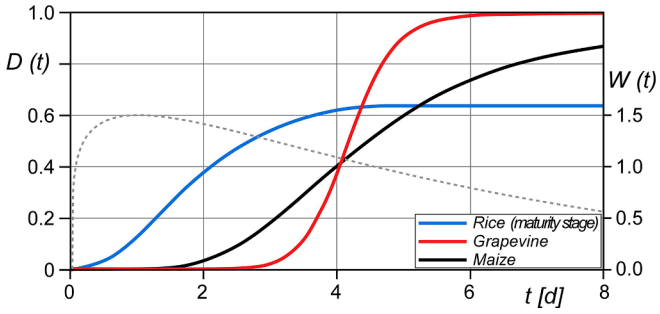

Fig. 8. Time evolution of the specific damage, $D(t)$, (solid lines) for rice (blue), grapevine (red), and maize (black), at the maturity stage, subject to the flood hydrograph n. 4 of Fig. 3 with $t_{max} = 1$ day and $W_{max} = 1.5$ (grey dashed line). (For interpretation of the references to colour in this figure legend, the reader is referred to the web version of this article.)

higher value of p (not reported here). Again, the persistence of flood plays a major role in determining the growth of damage.

3.2. Flood damage to residential buildings

Flood duration is one of the most important factors, together with water depth and flow velocity, also in assessing damage to residential buildings (Carisi et al., 2018; Chen et al., 2016; Grahn and Nyberg, 2014; Kellermann et al., 2020; Kelman and Spence, 2004; Martínez-Gomariz et al., 2020; Merz et al., 2013). Indeed, both structures and contents are typically made of porous materials; therefore, the longer is the flood duration, the more is the water absorbed, and the greater is the damage (Marvi, 2020; Nofal et al., 2020; Soetanto and Proverbs, 2004).

In this example, we use relative damage data provided by the 'what if' synthetic damage model INSYDE (Dottori et al., 2016; Molinari and Scorzini, 2017) forced by a set of couples (U, Y) lasting different durations, τ. In this case, the use of a 'what-if' model is appropriate, since we need values of damage for the same building but for different flood durations, and these values are not directly available from experimental data.

Differently from the previous example, in this case the structure of the impact parameter W is not known and must be assessed. Since the energy head, as well as the flow depth, are suitable flood impact parameters for reliable forecasting of damage to residential buildings (Kreibich et al., 2009; Lazzarin et al., 2022), we assume $\alpha = 1$ in Eq. (1) and chose $Y_W = 3.5$ m (i.e., approximately the typical inter-floor height) as reference depth, so that β remains the only calibration factor.

The vulnerability $V(W)$ is here defined as the damage produced by a constant hydrodynamic forcing, W, lasting for a sufficiently long time; in other words, $V(W)$ is the asymptotic value of the specific damage $D(t)$ considering the flood-event time scale. Accordingly, to calibrate β, we use a sub-set of the damage values provided by the INSYDE model; in particular, we consider the damage produced by velocity and flow depth couples lasting $\tau \approx 60$ h so that $D(W) \approx V(W)$. Since iso-V lines in the U—Y plane are also iso-W lines, we find β through a best-fit procedure, such that the shape of iso-W lines matches the shape of iso-V lines as well as possible. This procedure is detailed in Lazzarin et al. (2022).

Once the parameter W is assessed, we use the full set of data to construct a series of couples (W, D) for each duration τ. Hereafter, the procedure is the same as that described in the previous application (Sect. 3.1).

As an example, we consider a concrete 2-storey building with a footprint area of 100 m^2. In this case, we find $\beta = 0.3$ and the (W, D) couples plotted in Fig. 9a. For each duration τ, we then draw a continuous damage curve $D(W)$ from the set of couples (W, D). The large scatter of computed damage around the curves are mainly because INSYDE considers a stepwise effect of flood duration; in particular, the flood duration starts affecting the damage at $\tau = 30$ h and reaches its maximum effect at $\tau = 42$ h; this is the reason why the damage predicted by the model is constant when the duration is in the ranges $\tau \leq 30$ h and $\tau \geq 42$ h (Fig. 9b).

We use the curves of Fig. 9a to extract a set of points $D(\tau, W)$ for some values of the impact parameter, W ($0 \leq W \leq 1$ at a constant step $\Delta W = 0.2$) and for durations $\tau \leq 60$ h, at a constant step of 6 h (Fig. 9b). These points are then fitted by Eq. (6) to give $\gamma = 1.0$ and the values of vulnerability and damage rate factor reported in Table 2 and plotted in Fig. 9.

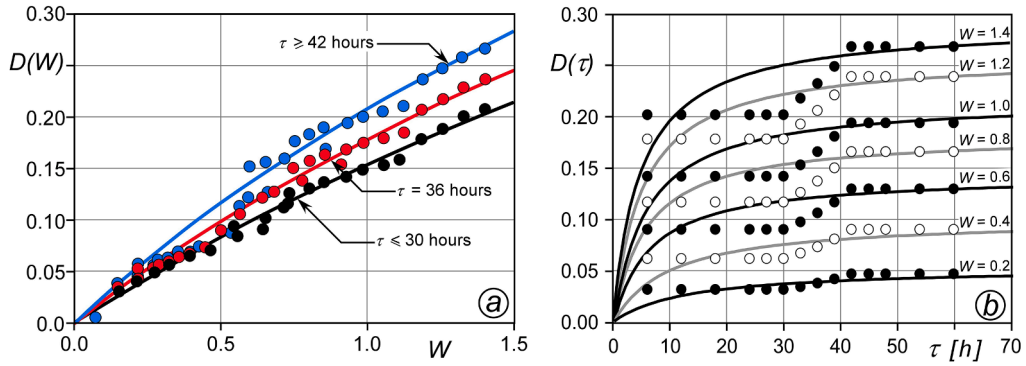

Fig. 9. Damage curves $D(W)$ for a concrete 2-storey building for different flood duration τ. b) Damage as a function of flood duration for different constant values of W; dots denote discrete values of $D(\tau, W)$ extracted from the curves plotted in panel a), whereas the curves are given by Eq. (6) with $t = \tau$.

Table 2
Model parameters V and c for a 2-storey concrete building for different values of the impact parameter W.

W	0.2	0.4	0.6	0.8	1.0	1.2	1.4
V	0.053	0.100	0.143	0.182	0.217	0.258	0.289
c [h^{-1}]	0.004	0.010	0.022	0.032	0.038	0.050	0.059

Here too, the large scatter of computed values/data around the interpolating iso-W curves of Fig. 9b is mainly ascribable to the stepped impact of the flood duration considered in the INSYDE model.

Vulnerability and damage rate factor values given in Table 2 could be interpolated using Eqs. (7) and (8), respectively. However, when the upper limit of vulnerability, $V = 100\%$ in Eq. (7), is far from being reached, as in the present case, a simpler power law like Eq. (9) can be used to interpolate the data (Fig. 10).

$$V(W) = bW^a \tag{9}$$

For the present case, we find $a = 0.8$, $b = 0.22$ and $p = 0.04\ h^{-1}$, $q = 1.3$.

The calibrated model is used to estimate the damage produced by the flood hydrographs of Fig. 3, with $t_{max} = 1$ h and $W_{max} = 1$. Numerical integration of Eq. (5), with boundary condition $D = 0$ at $t = 0$, yields the results shown in Fig. 11a. Even though the peak value of the impact parameter is the same for the four scenarios, the damage at the end of the flood event varies with the hydrograph shape significantly. With the hydrograph n. 4, which is characterized by the longer duration, the final damage is roughly doubled if compared with results obtained using the shortest hydrograph n. 1. This confirms the importance of considering the time evolution of the flood.

The above calibration procedure is applied also to the cases of concrete 1-storey and masonry 1- and 2- storey buildings; Fig. 11b-d shows the results of the model application. For each building, the damage evolution depends on the hydrograph shape only slightly up to $t = 2$ h; however, after the flood peak, the damage is strongly affected by the shape of the hydrograph. Again, the final damage for hydrograph n. 4 is approximatively two times the final damage for hydrograph n. 1.

Fig. 11 also shows that, for equivalent hydrodynamic forcing, the specific damage $D(t)$ is larger for 1-storey buildings (panels b and d) then for 2-storey buildings (panels a and c). This is because the vulnerability $V(W)$, which in turn depends on the number of floors and the building structure (e.g., masonry 1-floor buildings are more vulnerable than concrete 2-floors building), is higher for 1-storey buildings.

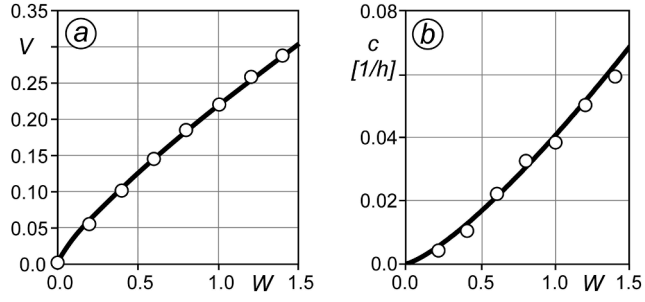

Fig. 10. Vulnerability $V(W)$ and damage rate factor $c(W)$ according to Eqs. (7) and (8), respectively, with $a = 0.8$, $b = 0.22$, and $p = 0.04\ h^{-1}$, $q = 1.3$. White dots denote the (V, W) and (c, W) couples of Table 2.

3.3. Flood damage to people

A significant category in the class of on/off objects is that of people. Many experimental data are available to calibrate the model, in the form of (U, Y) couples associated to off events. As a preliminarily step, the structure of the impact parameter is assessed by imposing that the iso-W line in the U—Y plane, corresponding to $W = 1$, well envelops 95% of the off events (i.e., 95% of off events have $W \leq 1$). We find $\alpha = 2$, $\beta = 4$, and $Y_w = 1.25$ m (additional details can be found in Lazzarin et al., 2022).

For classes of on/off objects, vulnerability is the probability of having an off event (Lazzarin et al., 2022); accordingly, $V(W)$ is given by the cumulative distribution function (CDF) of W associated to the off-events. In practical applications, it is often convenient to interpolate the (W, V) couples of discrete CDFs with an analytical function; to this purpose, Eq. (7) turns out to be simple and effective for different kind of on/off objects. In the example at hand, for the coefficients of Eq. (7), we find $a = 0.6$ and $b = 5.0$ (Fig. 12a).

As regards the damage rate factor, $c(W)$, it has to be admitted that suitable data and theoretical models are unavailable to describe the time dependence of the probability that a person is swept away by floodwaters for given hydrodynamic forcing. Accordingly, $c(W)$ must be assumed sensibly. However, the damaging process for people is typically fast compared to the flooding time scale, so that approximations affecting the estimating of $c(W)$ have a minor impact on the accuracy of model predictions. To show this, we assume that $c(W)$ is given by Eq. (8) with $q = 2$, and consider some values of the parameter p that, to a reasonable extent, represent different rates at which damage progresses. Fig. 12b shows the time course of the probability of occurrence of an off-event conditional to a constant $W = 1$ hydrodynamic forcing, and $p = 10, 25, 50\ h^{-1}$. In other words, Fig. 12b, shows how long floodwaters, characterized by $W = 1$, take to sweep away 95% of exposed adults, or how long an adult can roughly cope with floodwaters characterized by $W = 1$ before being swept away. According to the equation chosen for $c(W)$, this time is approximately 10 min, 30 min, and 1 h for $p = 50, 25, 10\ h^{-1}$, respectively. We then apply the model considering the steepest hydrograph of Fig. 3 (i.e., n. 1) and assume $W_{max} = 1$ and $t_{max} = 1$ h. Fig. 12c compares the vulnerability $V(t)$ with the damage $D(t)$ for the three values of p; the final damage, that exactly corresponds to the point

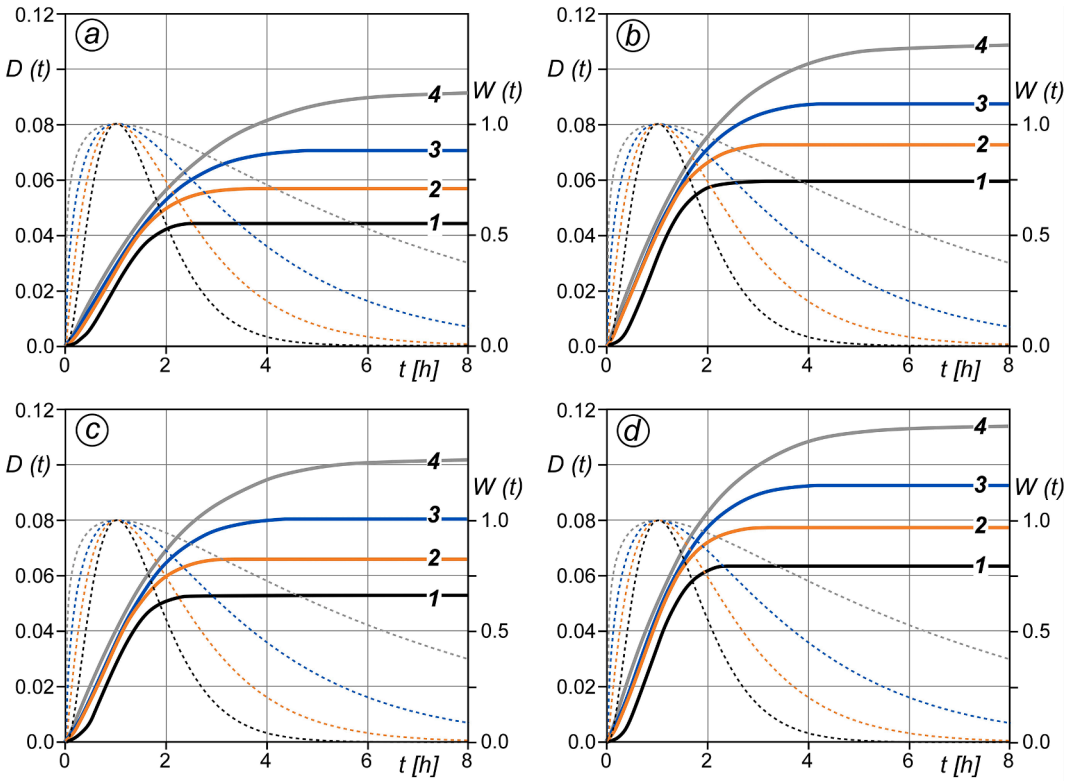

Fig. 11. Time evolution of the specific damage, $D(t)$, (solid lines) caused by the flood hydrographs $W(t)$ of Fig. 3 (dashed lines) with $t_{max} = 1$ h and $W_{max} = 1$, for a) concrete 2-storey building, b) concrete 1-storey building, c) masonry 2-storey building, d) masonry 1-storey building.

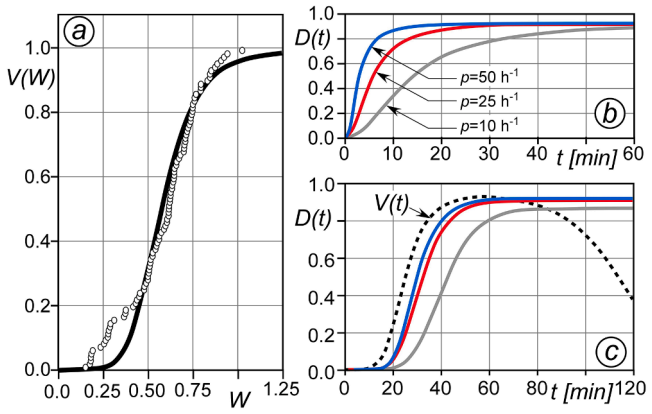

Fig. 12. a) Cumulative frequency distribution of off-events, $V(W)$, for the case of people in floodwaters; dots denote the available experimental data, the curve is given by Eq. (7) with $a = 0.6$ and $b = 5.0$ (adapted from Lazzarin et al., 2022). b) Specific damage as a function of time for constant forcing $W = 1$ and for $q = 2$, and three different values for p in Eq. (8). c) Damage as a function of time when the forcing is given by the hydrograph n. 1 in Fig. 3, and with the damage rate factor given by Eq. (8) with $q = 2$, and different values for p; the dashed curve is the corresponding vulnerability $V(t)$.

of intersection between $V(t)$ and $D(t)$, is not much smaller than the maximum possible damage, $D_{max} = V_{max} = V(W_{max})$. This holds even in the very improbable case of $p = 10$ h $^{-1}$, in which a person exposed to a very hazardous hydrodynamic condition (i.e., $W = 1$) would resist for more than one hour before being swept away. This behaviour confirms that an accurate assessing of $c(W)$ for the category of people and, possibly, for most of on/off categories, is important but not crucial in determining the accuracy of the model.

3.4. Additional remarks

To apply the proposed model, the key point is the calibration of γ and the estimation of the vulnerability function, V, and damage growth rate factor, c. In the present formulation of the model, both V and c only depend on the intensity of the hydrodynamic forcing, W. The vulnerability, $V(W)$, which is here defined as the potential damage produced in a sufficiently long period by a given hazard degree, is very similar to the specific damage estimated by classical models. In the present time-dependent approach, $V(W)$ modulates in time the damage growth. The damage rate factor, $c(W)$, expresses in mathematical form the idea that the flood damage develops at a rate that increases with the hazard. The previous model applications showed that a significant amount of data is needed to assess $c(W)$. For on/off items such as people exposed to floodwaters, available data is almost useless to determine $c(W)$; nonetheless, the model application suggests that, when the damaging process is fast compared to the flooding time scale (as it is for people), even large uncertainties on $c(W)$ have a minor impact on the accuracy of model prediction. In other words, for item category subject to fast damaging, the present model remains useful to track the time-evolution of damage, which is essentially driven by the time variation of hazard, and to consider the effect of countermeasures and rescue activities undertaken during the course of the flood event.

For items subject to progressive damaging, the schematic applications shown above suggest that considering the real time evolution of the flood event is key for reliable damage estimation. In the model applications to crops and buildings (Figs. 6, 8, and 11), the specific damage is still very low at the time of the flood peak, and mainly develops during the receding phase of the flood. The peak flood condition alone, as well as long-standing shallow water depths, can play a minor role in determining the final damage. This means that the successful application of the classic approach for damage estimation requires defining and estimating hazard indicators (i.e., an effective equivalent water depth, and an effective equivalent flood duration) that are truly representative of

the time-varying flood conditions. This is not straightforward, and can be especially challenging when the shape of the flood hydrograph is very irregular as, e.g., in the case of multi-peak hydrographs. This issue is overcome in the time-dependent framework here proposed, which naturally accounts for the time evolution of damage during the flood, thus retaining the full information of the damaging states contained in a flood hydrograph.

The effectiveness of the method is intimately related to the use of numerical flood models, typically based on the shallow water equations, which are now consolidated tools in supporting flood damage and flood risk analyses (Costabile et al., 2020; Ernst et al., 2010; Ferrari et al., 2019, Ferrari and Viero, 2020; Jamali et al., 2018; Sanders and Schubert, 2019; Teng et al., 2017; Viero et al., 2019). These models provide water depth and velocity at each time-step and at each point of the flooded area, and hence the time course and spatial distribution of the impact parameter W. At each computational grid point, time integration of Eq. (5) can advance simultaneously with the hydrodynamic model to provide the spatial distribution of the damage $D(\mathbf{x}, t)\bullet\mathbb{E}(\mathbf{x}, t)$. The latter, once the flood receded, gives the spatial distribution of the flood damage.

4. Conclusions

The present work introduces a new framework for flood damage assessment, which considers the time evolution of the entire damaging process within a single flood event. This is a new perspective, since the many models for flood damage assessment developed up to now, either physics- or data-based, uni- or multi-variate, deterministic or probabilistic, correlate the damage produced by a flood event to some summary indicators of hazard and exposure, thus disregarding the time course of the flood event and of the processes that lead to flood damage.

A logistic-type equation is here chosen to predict, at each point within the flooded area, the time evolution of damage driven by the time-varying features of the flood event, accounting for the fractions of damaged, exposed, vulnerable, and possibly rescued items. The total damage is then obtained through spatial integration over the flooded area.

Model applications to crops, residential buildings, and people exposed to floodwaters are used to show how to assess the model parameters and functions based on available data, and to demonstrate some of the advantage of the proposed approach. Specifically, the model allows to assess flood damage of different asset categories, yet retaining a common structure; i.e., the different damage processes are described by the same equations and just different values of the calibration parameters. The duration of the flood event is accounted for implicitly and effectively, and the strong hypothesis that the final damage may be completely described by a limited set of characteristic parameters, such as the maximum water depth and flow velocity, is relaxed. Importantly, the main model components have a precise physical meaning, which is of help to the modelers in case data or synthetic models are scarce or unavailable.

Although further research is definitely needed to obtain a reliable model applicable to real-world general cases, the proposed framework suggests a different point of view in flood risk assessment, closer to the damaging processes that actually occur during a flood, and paves the way to a set of innovative applications towards a more effective flood risk assessment and management.

The proposed approach also allows to account for the impact of countermeasures and of rescue activities that may be undertaken during the flood event, aimed at reducing the exposed items. This aspect is not analyzed in the paper mainly because of the many diverse factors on which rescue activities depend on, including the availability and efficiency of rescue services, the quantity of items to be rescued, and the hydrodynamic forcing as well. Accounting for the mutual feedbacks between the emergency rescue activities and the dynamics of hazard and damage, requires the coupling of the damage and hydrodynamic models. This occurrence suggests the opportunity of coupling of the present model for time-dependent flood damage with available or advanced versions of agent-based models (e.g., Dawson et al., 2011; Zhuo and Han, 2020), which can provide effective estimates of the rescue function, R, for on/off, fast damaging item categories like people and cattle. Rescue activities are expected to play a key role also for long and slowly varying flood events, for which the quantity of exposed assets can decrease because of rescue activities performed by civil protection actors or citizens (like evacuating people and cattle, moving vulnerable contents at upper level, etc.). Disregarding the fraction of assets that can actually be rescued or moved during such flood events, may lead to significant overestimations of damage.

As for further future activities, model application to significant real cases, having sufficiently accurate data of both the hydrodynamic and damaging processes of a few categories, is needed to more clearly demonstrate the efficacy of the proposed approach. Furthermore, the general time-dependent framework here proposed could be useful for modelling other time-dependent flood-related processes (e.g., soil alteration, biological degradation, indirect damages, business interruption, etc.), possibly including additional or different damage determinants (e.g., pollutants).

Funding

This research did not receive any specific grant from funding agencies in the public, commercial, or not-for-profit sectors.

Data statement

The data on which this article is based are available in the cited literature.

CRediT authorship contribution statement

Tommaso Lazzarin: Conceptualization, Methodology, Investigation, Visualization, Writing – original draft. **Daniele P. Viero:** Methodology, Writing – review & editing. **Daniela Molinari:** Methodology, Writing – review & editing. **Francesco Ballio:** Methodology, Writing – review & editing. **Andrea Defina:** Conceptualization, Visualization, Writing – review & editing, Supervision.

Declaration of Competing Interest

The authors declare that they have no known competing financial interests or personal relationships that could have appeared to influence the work reported in this paper.

Data availability

The data on which this article is based are available in the cited literature.

References

Agenais, A.L., Grelot, F., Brémond, P., Erdlenbruch, K., 2013. Dommages des inondations au secteur agricole: guide méthodologique et fonctions nationales. IRSTEA 321. https://hal.inrae.fr/hal-02600061.

Arrighi, C., Alcèrreca-Huerta, J.C., Oumeraci, H., Castelli, F., 2015. Drag and lift contribution to the incipient motion of partly submerged flooded vehicles. J. Fluids Struct. 57, 170–184. https://doi.org/10.1016/j.jfluidstructs.2015.06.010.

Arrighi, C., Oumeraci, H., Castelli, F., 2017. Hydrodynamics of pedestrians' instability in floodwaters. Hydrol. Earth Syst. Sci. 21, 515–531. https://doi.org/10.5194/hess-21-515-2017.

Arrighi, C., Brugioni, M., Castelli, F., Franceschini, S., Mazzanti, B., 2018. Flood risk assessment in art cities: the exemplary case of Florence (Italy). J. Flood Risk Manag. 11, S616–S631. https://doi.org/10.1111/jfr3.12226.

Berning, C., Viljoen, M., Plessis, L., 2000. Loss functions for sugar-cane: depth and duration of inundation as determinants of extent of flood damage. Water SA 26, 527–530.

Bocanegra, R.A., Vallés-Morán, F.J., Francés, F., 2020. Review and analysis of vehicle stability models during floods and proposal for future improvements. J. Flood Risk Manag. 13, e12551 https://doi.org/10.1111/jfr3.12551.
Breaden, J.P., 1971. The Generation of Flood Damage Time Sequences. KWRRI Research Reports. https://doi.org/10.13023/kwrri.rr.32.
Brémond, P., Grelot, F., Agenais, A.-L., 2013. Review article: economic evaluation of flood damage to agriculture – review and analysis of existing methods. Nat. Hazards Earth Syst. Sci. 13, 2493–2512. https://doi.org/10.5194/nhess-13-2493-2013.
Carisi, F., Schröter, K., Domeneghetti, A., Kreibich, H., Castellarin, A., 2018. Development and assessment of uni- and multivariable flood loss models for Emilia-Romagna (Italy). Nat. Hazards Earth Syst. Sci. 18, 2057–2079. https://doi.org/10.5194/nhess-18-2057-2018.
Chapman, E.J., Byron, C.J., 2018. The flexible application of carrying capacity in ecology. Glob. Ecol. Conserv. 13, e00365 https://doi.org/10.1016/j.gecco.2017.e00365.
Chen, A.S., Hammond, M.J., Djordjević, S., Butler, D., Khan, D.M., Veerbeek, W., 2016. From hazard to impact: flood damage assessment tools for mega cities. Nat. Hazards 82, 857–890. https://doi.org/10.1007/s11069-016-2223-2.
Costabile, P., Costanzo, C., De Lorenzo, G., Macchione, F., 2020. Is local flood hazard assessment in urban areas significantly influenced by the physical complexity of the hydrodynamic inundation model? J. Hydrol. 580, 124231 https://doi.org/10.1016/j.jhydrol.2019.124231.
Cox, R.J., Shand, T.D., Blacka, M.J., 2010. Australian Rainfall and Runoff (AR&R). Revision Project 10: Appropriate Safety Criteria for People. Department of Infrastructures Planning and Natural Resources, NSW. https://doi.org/10.1038/103447b0.
Dawson, R.J., Peppe, R., Wang, M., 2011. An agent-based model for risk-based flood incident management. Nat. Hazards 59, 167–189. https://doi.org/10.1007/s11069-011-9745-4.
Dottori, F., Figueiredo, R., Martina, M.L.V., Molinari, D., Scorzini, A.R., 2016. INSYDE: a synthetic, probabilistic flood damage model based on explicit cost analysis. Nat. Hazards Earth Syst. Sci. 16, 2577–2591. https://doi.org/10.5194/nhess-16-2577-2016.
Dutta, D., Herath, S., Musiake, K., 2003. A mathematical model for flood loss estimation. J. Hydrol. 277, 24–49. https://doi.org/10.1016/S0022-1694(03)00084-2.
Ernst, J., Dewals, B.J., Detrembleur, S., Archambeau, P., Erpicum, S., Pirotton, M., 2010. Micro-scale flood risk analysis based on detailed 2D hydraulic modelling and high resolution geographic data. Nat. Hazards 55, 181–209. https://doi.org/10.1007/s11069-010-9520-y.
Ferrari, A., Viero, D.P., 2020. Floodwater pathways in urban areas: a method to compute porosity fields for anisotropic subgrid models in differential form. J. Hydrol. 589, 125193 https://doi.org/10.1016/j.jhydrol.2020.125193.
Ferrari, A., Viero, D.P., Vacondio, R., Defina, A., Mignosa, P., 2019. Flood inundation modeling in urbanized areas: a mesh-independent porosity approach with anisotropic friction. Adv. Water Resour. 125, 98–113. https://doi.org/10.1016/j.advwatres.2019.01.010.
Figueiredo, R., Romão, X., Paupério, E., 2021. Component-based flood vulnerability modelling for cultural heritage buildings. Int. J. Disaster Risk Reduct. 61, 102323 https://doi.org/10.1016/j.ijdrr.2021.102323.
Forster, S., Kuhlmann, B., Lindenschmidt, K.E., Bronstert, A., 2008. Assessing flood risk for a rural detention area. Nat. Hazards Earth Syst. Sci. 8, 311–322. https://doi.org/10.5194/nhess-8-311-2008.
Gallazzi, A., Molinari, D., Ballio, F., Scorzini, A.R., 2021. Development of a flood damage model for urban drainage networks. In: Proceedings of FLOODrisk 2020 - 4th European Conference on Flood Risk Management. https://doi.org/10.3311/FloodRisk2020.6.2. Online.
Gerl, T., Kreibich, H., Franco, G., Marechal, D., Schröter, K., 2016. A review of flood loss models as basis for harmonization and benchmarking. PLoS One 11, e0159791. https://doi.org/10.1371/journal.pone.0159791.
Gissing, A., Blong, R., 2004. Accounting for variability in commercial flood damage estimation. Aust. Geogr. 35, 209–222. https://doi.org/10.1080/0004918042000249511.
Grahn, T., Nyberg, R., 2014. Damage assessment of lake floods: insured damage to private property during two lake floods in Sweden 2000/2001. Int. J. Disaster Risk Reduct. 10, 305–314. https://doi.org/10.1016/j.ijdrr.2014.10.003.
Jamali, B., Löwe, R., Bach, P.M., Urich, C., Arnbjerg-Nielsen, K., Deletic, A., 2018. A rapid urban flood inundation and damage assessment model. J. Hydrol. 564, 1085–1098. https://doi.org/10.1016/j.jhydrol.2018.07.064.
Jonkman, S.N., Penning-Rowsell, E., 2008. Human instability in flood flows. JAWRA J. Am. Water Resour. Assoc. 44, 1208–1218. https://doi.org/10.1111/j.1752-1688.2008.00217.x.
Kellermann, P., Schröter, K., Thieken, A.H., Haubrock, S.-N., Kreibich, H., 2020. The object-specific flood damage database HOWAS 21. Nat. Hazards Earth Syst. Sci. 20, 2503–2519. https://doi.org/10.5194/nhess-20-2503-2020.
Kelman, I., Spence, R., 2004. An overview of flood actions on buildings. Eng. Geol. 73, 297–309. https://doi.org/10.1016/j.enggeo.2004.01.010.
Khairul, I.M., Rasmy, M., Ohara, M., Takeuchi, K., 2022. Developing flood vulnerability functions through questionnaire survey for flood risk assessments in the Meghna Basin, Bangladesh. Water Switz. 14, 369. https://doi.org/10.3390/w14030369.
Kienzler, S., Pech, I., Kreibich, H., Müller, M., Thieken, A.H., 2015. After the extreme flood in 2002: changes in preparedness, response and recovery of flood-affected residents in Germany between 2005 and 2011. Nat. Hazards Earth Syst. Sci. 15, 505–526. https://doi.org/10.5194/nhess-15-505-2015.
Kramer, M., Terheiden, K., Wieprecht, S., 2016. Safety criteria for the trafficability of inundated roads in urban floodings. Int. J. Disaster Risk Reduct. 17, 77–84. https://doi.org/10.1016/j.ijdrr.2016.04.003.
Kreibich, H., Piroth, K., Seifert, I., Maiwald, H., Kunert, U., Schwarz, J., Merz, B., Thieken, A.H., 2009. Is flow velocity a significant parameter in flood damage modelling? Nat. Hazards Earth Syst. Sci. 9, 1679–1692. https://doi.org/10.5194/nhess-9-1679-2009.
Kreibich, H., Seifert, I., Merz, B., Thieken, A.H., 2010. Development of FLEMOcs – a new model for the estimation of flood losses in the commercial sector. Hydrol. Sci. J. 55, 1302–1314. https://doi.org/10.1080/02626667.2010.529815.
Kreibich, H., Botto, A., Merz, B., Schröter, K., 2017. Probabilistic, multivariable flood loss modeling on the mesoscale with BT-FLEMO. Risk Anal. 37, 774–787. https://doi.org/10.1111/risa.12650.
Lazzarin, T., Viero, D.P., Molinari, D., Ballio, F., Defina, A., 2022. Flood damage functions based on a single physics- and data-based impact parameter that jointly accounts for water depth and velocity. J. Hydrol. 607, 127485 https://doi.org/10.1016/j.jhydrol.2022.127485.
Lind, N., Hartford, D., Assaf, H., 2004. Hydrodynamic models of human instability in a flood. J. Am. Water Resour. Assoc. 8, 89–96.
Lüdtke, S., Schröter, K., Steinhausen, M., Weise, L., Figueiredo, R., Kreibich, H., 2019. A consistent approach for probabilistic residential flood loss modeling in Europe. Water Resour. Res. 55, 10616–10635. https://doi.org/10.1029/2019WR026213.
Mao, G., Onfroy, T., Moncoulon, D., Quantin, A., Robert, C., 2016. Comprehensive flood economic losses: review of the potential damage and implementation of an agricultural impact model. 3rd Eur. Conf. Flood Risk Manag. FLOODrisk 2016 (7), 05003. https://doi.org/10.1051/e3sconf/20160705003.
Martínez-Gomariz, E., Gómez, M., Russo, B., Djordjević, S., 2018. Stability criteria for flooded vehicles: a state-of-the-art review. J. Flood Risk Manag. 11, S817–S826. https://doi.org/10.1111/jfr3.12262.
Martínez-Gomariz, E., Forero-Ortiz, E., Guerrero-Hidalga, M., Castán, S., Gómez, M., 2020. Flood depth-damage curves for Spanish urban areas. Sustain. Switz. 12, 2666. https://doi.org/10.3390/su12072666.
Marvi, M.T., 2020. A review of flood damage analysis for a building structure and contents. Nat. Hazards 102 (3), 967–995. https://doi.org/10.1007/s11069-020-03941-w.
Merz, B., Kreibich, H., Schwarze, R., Thieken, A., 2010. Assessment of economic flood damage. Nat. Hazards Earth Syst. Sci. 10, 1697–1724. https://doi.org/10.5194/nhess-10-1697-2010.
Merz, B., Kreibich, H., Lall, U., 2013. Multi-variate flood damage assessment: a tree-based data-mining approach. Nat. Hazards Earth Syst. Sci. 13, 53–64. https://doi.org/10.5194/nhess-13-53-2013.
Milanesi, L., Pilotti, M., 2019. A conceptual model of vehicles stability in flood flows. J. Hydraul. Res. 58 (4), 701–708. https://doi.org/10.1080/00221686.2019.1647887.
Milanesi, L., Pilotti, M., Ranzi, R., 2015. A conceptual model of people's vulnerability to floods. Water Resour. Res. 51, 182–197. https://doi.org/10.1002/2014WR016172.
de Moel, H., Aerts, J.C.J.H., 2011. Effect of uncertainty in land use, damage models and inundation depth on flood damage estimates. Nat. Hazards 58 (1), 407–425. https://doi.org/10.1007/s11069-010-9675-6.
Molinari, D., Scorzini, A.R., 2017. On the influence of input data quality to flood damage estimation: the performance of the INSYDE model. Water Switz. 9 (9), 688. https://doi.org/10.3390/w9090688.
Molinari, D., Scorzini, A.R., Gallazzi, A., Ballio, F., 2019. AGRIDE-c, a conceptual model for the estimation of flood damage to crops development and implementation. Nat. Hazards Earth Syst. Sci. 19, 2565–2582. https://doi.org/10.5194/nhess-19-2565-2019.
Nguyen, N.Y., Kha, D.D., Ichikawa, Y., 2021. Developing a multivariable lookup table function for estimating flood damages of rice crop in Vietnam using a secondary research approach. Int. J. Disaster Risk Reduct. 58, 102208 https://doi.org/10.1016/j.ijdrr.2021.102208.
Nofal, O.M., van de Lindt, J.W., Do, T.Q., 2020. Multi-variate and single-variable flood fragility and loss approaches for buildings. Reliab. Eng. Syst. Saf. 202, 106971 https://doi.org/10.1016/j.ress.2020.106971.
Pita, G.L., Albornoz, B.S., Zaracho, J.I., 2021. Flood depth-damage and fragility functions derived with structured expert judgment. J. Hydrol. 603, 126982 https://doi.org/10.1016/j.jhydrol.2021.126982.
Pregnolato, M., Ford, A., Wilkinson, S.M., Dawson, R.J., 2017. The impact of flooding on road transport: a depth-disruption function. Transp. Res. Part Transp. Environ. 55, 67–81. https://doi.org/10.1016/j.trd.2017.06.020.
Ramsbottom, D., Wade, S., Bain, V., 2006. Flood Risks to People - Phase 2 - FD2321/TR2 Guidance Document. Flood Hazard Res. Cent. Middx. Univ.
Sairam, N., Schröter, K., Carisi, F., Wagenaar, D., Domeneghetti, A., Molinari, D., Brill, F., Priest, S., Viavattene, C., Merz, B., Kreibich, H., 2020. Bayesian data-driven approach enhances synthetic flood loss models. Environ. Model. Softw. 132, 104798 https://doi.org/10.1016/j.envsoft.2020.104798.
Samantaray, D., Chatterjee, C., Singh, R., Gupta, P.K., Panigrahy, S., 2015. Flood risk modeling for optimal rice planning for delta region of Mahanadi river basin in India. Nat. Hazards 76, 347–372. https://doi.org/10.1007/s11069-014-1493-9.
Sanders, B.F., Schubert, J.E., 2019. PRIMo: Parallel raster inundation model. Adv. Water Resour. 126, 79–95. https://doi.org/10.1016/j.advwatres.2019.02.007.
Scawthorn, C., Asce, F., Flores, P., Blais, N., Seligson, H., Tate, E., Chang, S., Mifflin, E., Thomas, W., Murphy, J., Jones, C., Lawrence, M., 2006. HAZUS-MH flood loss estimation methodology. II. Damage and loss assessment. Nat. Hazards Rev. 7, 72–81. https://doi.org/10.1061/(ASCE)1527-6988(2006)7:2(72).
Schröter, K., Kreibich, H., Vogel, K., Riggelsen, C., Scherbaum, F., Merz, B., 2014. How useful are complex flood damage models? Water Resour. Res. 50, 3378–3395. https://doi.org/10.1002/2013WR014396.

Shand, T.D., Cox, R.J., Blacka, M.J., Smith, G.P., 2011. Australian rainfall and runoff (AR&R). Revision project 10: appropriate safety criteria for vehicles. Rep. Number P10S2020.

Shrestha, B.B., Okazumi, T., Miyamoto, M., Sawano, H., 2016. Flood damage assessment in the Pampanga river basin of the Philippines. J. Flood Risk Manag. 9, 355–369. https://doi.org/10.1111/jfr3.12174.

Singh, S., Mackill, D.J., Ismail, A.M., 2011. Tolerance of longer-term partial stagnant flooding is independent of the SUB1 locus in rice. Field Crops Res. 121, 311–323. https://doi.org/10.1016/j.fcr.2010.12.021.

Soetanto, R., Proverbs, D.G., 2004. Impact of flood characteristics on damage caused to UK domestic properties: the perceptions of building surveyors. Struct. Surv. 22, 95–104. https://doi.org/10.1108/02630800410538622.

Teng, J., Jakeman, A.J., Vaze, J., Croke, B.F.W., Dutta, D., Kim, S., 2017. Flood inundation modelling: a review of methods, recent advances and uncertainty analysis. Environ. Model. Softw. 90, 201–216. https://doi.org/10.1016/j.envsoft.2017.01.006.

Thieken, A.H., Kreibich, H., Müller, M., Merz, B., 2007. Coping with floods: preparedness, response and recovery of flood-affected residents in Germany in 2002. Hydrol. Sci. J. 52, 1016–1037. https://doi.org/10.1623/hysj.52.5.1016.

Viero, D.P., Roder, G., Matticchio, B., Defina, A., Tarolli, P., 2019. Floods, landscape modifications and population dynamics in anthropogenic coastal lowlands: the Polesine (northern Italy) case study. Sci. Total Environ. 651, 1435–1450. https://doi.org/10.1016/j.scitotenv.2018.09.1214.

Vozinaki, A.-E.K., Karatzas, G.P., Sibetheros, I.A., Varouchakis, E.A., 2015. An agricultural flash flood loss estimation methodology: the case study of the Koiliaris basin (Greece), February 2003 flood. Nat. Hazards 79, 899–920. https://doi.org/10.1007/s11069-015-1882-8.

Wagenaar, D., de Jong, J., Bouwer, L.M., 2017. Multi-variable flood damage modelling with limited data using supervised learning approaches. Nat. Hazards Earth Syst. Sci. 17, 1683–1696. https://doi.org/10.5194/nhess-17-1683-2017.

White, G.F., 1945. Human Adjustment to Floods: A Geographical Approach to the Flood Problem in the United States. Univ. Chic. Dept Geogr. Research Paper No.29.

White, G.F., 1964. Choice of adjustment to floods. Univ. Chic. Dept Geogr. Research Paper No.93.

Zhang, Y., Wang, Z., Li, L., Zhou, Q., Xiao, Y., Wei, X., Zhou, M., 2015. Short-term complete submergence of Rice at the Tillering stage increases yield. PLoS One 10, e0127982. https://doi.org/10.1371/journal.pone.0127982.

Zhuo, L., Han, D., 2020. Agent-based modelling and flood risk management: a compendious literature review. J. Hydrol. 591, 125600 https://doi.org/10.1016/j.jhydrol.2020.125600.